HHS Public Access

Author manuscript

Reprod Sci. Author manuscript; available in PMC 2023 May 07.

Published in final edited form as:

Reprod Sci. 2023 May ; 30(5): 1528–1539. doi:10.1007/s43032-022-01097-5.

AKAP13 Enhances CREB1 Activation by FSH in Granulosa Cells

Kamaria C. Cayton Vaught[1], **Dana Hazimeh**[2], **Ashlie Sewdass Carter**[1], **Kate Devine**[3,4], **Jacqueline Y. Maher**[1,5], **Marcy Maguire**[3,6], **Elizabeth A. McGee**[7], **Paul H. Driggers**[1], **James H. Segars**[1]

[1]Division of Reproductive Sciences & Women's Health Research, Department of Gynecology and Obstetrics, Johns Hopkins University School of Medicine, Baltimore, MD 21205, USA

[2]American University of Beirut Medical Centre, Beirut, Lebanon

[3]Section On Reproductive Endocrinology, Eunice Kennedy Shriver National Institute of Child Health and Human Development, National Institutes of Health, Bethesda, MD 20892, USA

[4]Shady Grove Fertility, Washington, DC 20006, USA

[5]Section On Pediatric and Adolescent Gynecology, Eunice Kennedy Shriver National Institute of Child Health and Human Development, National Institutes of Health, Bethesda, MD 20892, USA

[6]Reproductive Medicine Associates of New Jersey, West Orange, NJ 07052, USA

[7]Division of Reproductive Endocrinology, Department of Obstetrics, Gynecology, and Reproductive Medicine, University of Vermont, Burlington, VT 05405, USA

Abstract

Granulosa cells (GCs) must respond appropriately to follicle-stimulating hormone (FSH) for proper follicle maturation. FSH activates protein kinase A (PKA) leading to phosphorylation of the cyclic AMP response element binding protein-1 (CREB1). We identified a unique A-kinase anchoring protein (AKAP13) containing a Rho guanine nucleotide exchange factor (RhoGEF) region that was induced in GCs during folliculogenesis. AKAPs are known to coordinate signaling cascades, and we sought to evaluate the role of AKAP13 in GCs in response to FSH. Aromatase

✉Kamaria C. Cayton Vaught, Kcayton1@jhmi.edu.

Author Contribution All authors contributed to the study conception and design. Material preparation, data collection, and analysis were performed by Kamaria C. Cayton Vaught, Kate Devine, Ashlie Sewdass, Jacqueline Y. Maher, Dana Hazimeh, Marcy Maguire, Elizabeth A. McGee, Paul H. Driggers, and James H. Segars. The first draft of the manuscript was written by Kamaria C. Cayton Vaught and all authors commented on previous versions of the manuscript. All authors read and approved the final manuscript.

Conflict of Interest The authors declare no competing interests.

Data Availability Not applicable.

Code Availability Not applicable.

Declarations

Ethics Approval All experimental procedures involving animals were conducted in accordance with the Intuitional Animal Care and Use Committees at the National Institute of Health. Animals were cared for as per institutional regulations under the reviewed and approved animal study protocols, ASP 03-001, ASP 06-002, ASP 12-060, and ASP 15-060.

Consent to Participate Not applicable.

Consent for Publication Not applicable.

reporter activity was increased in COV434 human GCs overexpressing AKAP13. Addition of FSH, or the PKA activator forskolin, significantly enhanced this activity by 1.5- to 2.5-fold, respectively ($p < 0.001$). Treatment with the PKA inhibitor H89 significantly reduced AKAP13-dependent activation of an aromatase reporter ($p = 0.0067$). AKAP13 physically interacted with CREB1 in co-immunoprecipitation experiments and increased the phosphorylation of CREB1. CREB1 phosphorylation increased after FSH treatment in a time-specific manner, and this effect was reduced by siRNA directed against *AKAP13* ($p = 0.05$). CREB1 activation increased by 18.5-fold with co-expression of AKAP13 in the presence of FSH ($p < 0.001$). Aromatase reporter activity was reduced by inhibitors of the RhoGEF region, C3 transferase and A13, and greatly enhanced by the RhoGEF activator, A02. In primary murine and COV43 GCs, siRNA knockdown of *Akap13/AKAP13* decreased aromatase and luteinizing hormone receptor transcripts in cells treated with FSH, compared with controls. Collectively, these findings suggest that AKAP13 may function as a scaffolding protein in FSH signal transduction via an interaction with CREB, resulting in phosphorylation of CREB.

Keywords

AKAP13; Follicular maturation; FSH signaling; PKA signaling; CREB; Folliculogenesis

Introduction

Gonadotropin-dependent signaling in the ovary is essential for follicular development. A key event in follicular maturation is the transition of granulosa cells (GCs) from the preantral to the preovulatory state. This process involves the production of P450 aromatase (CYP19A1), which converts androstenedione to estrone, and the induction of the luteinizing hormone receptor (LHR), which is critical for ovulation.

The production of aromatase and LHR is follicle-stimulating hormone (FSH)-dependent and involves a protein kinase A (PKA)-mediated signaling cascade [1–4]. Specifically, FSH binds via a leucine-rich repeat (LRR) motif [5] to the FSH receptor (FSHR), a G-protein-coupled receptor located on the cell surface. This interaction results in the activation of adenylyl cyclase and increased formation of cyclic adenosine monophosphate (cAMP) [6–8]. Cyclic-AMP binds to the two regulatory (RI and RII) subunits of PKA, releasing its two active catalytic (C) subunits to phosphorylate serine-threonine residues on target substrates [9, 10]. The PKA RII subunit, specifically, is upregulated in response to FSH in the ovary [11–14]. The binding of cAMP has multiple effects, including phosphorylation of the transcription factor cAMP response element binding protein-1 (CREB1) [4]. Phosphorylation of CREB1 leads to the activation of numerous target genes, including *CYP19A1*. CREB1 activates a cAMP response element (CRE) in region B of the aromatase promoter, leading to increased aromatase production [15]. Although the responses of GCs to FSH are understood [1, 16–19], the role of all downstream regulatory molecules that interact with CREB1 is complex, and understanding of potential interacting proteins may suggest new tractable targets to regulate FSH signaling.

Our group previously cloned a full-length transcript of a novel gene known to regulate PKA, later called A-Kinase Anchoring Protein 13 *(AKAP13*) [20]. AKAP13 is a member of the AKAP family of proteins, which is comprised of over 40 functionally related genes notable for their multiple modular binding domains [21, 22]. This feature allows AKAP proteins to form multimeric complexes, thereby orchestrating a rapid and precise series of reactions to facilitate downstream outcomes of hormone signaling [9]. AKAP13 is expressed in multiple tissues and contains a PKA regulatory subunit II (PKA RII) binding domain at its N-terminal, a guanine nucleotide exchange factor (GEF) domain capable of binding Ras homolog family member A, RhoA [20, 23, 24], and a nuclear hormone receptor binding (LXXLL) domain at its C-terminal [25, 26]. Through these structural motifs, AKAP13 can form signaling complexes with RhoA and PKA, in addition to several hormones such as estradiol, progesterone, glucocorticoids, and various other signaling molecules. AKAP13 plays an essential role in cell development [20, 25–30] and was recently shown to be involved in translational initiation, mRNA nonsense-mediated decay, rRNA processing, and mRNA splicing [31].

AKAP13 is expressed in the cytoplasm of GCs in mature follicles, the corpus luteum, and hilar cells in the ovary [32–34]. We questioned whether AKAP13 might be involved in GC function and thus in FSH signaling, since both AKAP13 and type II PKA are induced in GCs during the follicular response to FSH [34, 35]. Our main objective was to evaluate the relationship between AKAP13 and CREB1 in FSH signaling in GCs. Utilizing primary murine and immortalized human GCs, we found that AKAP13 plays a role in follicular development through a direct physical interaction with CREB1, augmenting FSH-induced CREB1 phosphorylation and increasing the transcription of the *CYP19A1* and *LHR* genes. Optimal activation of CREB1 also required the RhoGEF region of AKAP13 suggesting a coordination of signaling between the PKA and Rho pathways.

Methods

Cell Lines

Primary Murine Granulosa Cell Culture—Animals were cared for as per institutional regulations under the reviewed and approved animal study protocols, ASP 03-001, ASP 06-002, ASP 12-060, and ASP 15-060. WT C57BL/6 mice were purchased from Jackson Laboratories. Whole ovaries were collected from 12 to 24-week-old mice following sacrifice and placed in phosphate-buffered saline with 1% penicillin/streptomycin (Invitrogen, Grand Island, NY). The ovaries were then incubated for 10 min in McCoy's 5A media (Sigma-Aldrich, St Louis, MO) containing ethyleneglycoltetracetic acid (Sigma-Aldrich) and sodium bicarbonate. Subsequently, the ovaries were transferred to a warmed solution consisting of 0.5 M sucrose and McCoy's 5A media. Lastly, the ovaries were transferred to a culture media composed of McCoy's 5A media, 10% fetal bovine serum (FBS), and 1% penicillin/streptomycin. GCs were released via antral follicle puncture, and ovarian "shells" were removed. Cells were stained with trypan blue to assess viability and were counted using a hemocytometer. The cells were then plated as described [36]. The cells were grown in McCoy's 5A media containing 10% fetal bovine serum and 1% penicillin/streptomycin

at 37 °F. The media was changed 24 h after cell harvest. In experiments employing siRNA, cells were cultured in Opti-MEM (Invitrogen) for 24 h prior to transfection.

COV434 Cell Culture—COV434 cells (Sigma-Aldrich, USA, #07,071,909) are a diploid immortalized human GC line derived from a GC tumor and have been demonstrated to be hormonally responsive [37, 38]. The COV434 cells were cultured in fresh DMEM/F12 media (Thermo Fisher Scientific, Waltham, MA) supplemented with 10% FBS (GIBCO by Life Technologies) with 1% penicillin/streptomycin (Millipore Sigma, USA, #P3032-10MU/ #S9137-25G) and 1% L-glutamine (Quantity Biological, USA) at 37 °C in 95% air and 5% CO2. Cells were stained with trypan blue (Sigma-Aldrich, USA) to assess viability and were counted using an automated cell counter (NanoEnTek Eve Automatic Cell Counter). For most experiments, the cells were plated on standard tissue cultured-treated polystyrene plates (Corning, USA) in varying well-size plates including 6 and 24 well plates. Seeding densities for 6 well plates were 6.0×10^5 cells/well and for 24 well plates, 2.0 to 2.5×10^5 cells/well.

Transfection of Primary Murine and Human COV434 Granulosa Cells

siRNA Transfection

Primary Murine Granulosa Cells: Cells were plated and incubated in McCoy's 5A culture medium as described above. When the cells were approximately 40–70% confluent, the medium was changed to Opti-MEM (Invitrogen) for 24 h. Lipofectamine 2000 (Invitrogen, catalog # 11,668–027) was then applied to the cells according to the manufacturer's protocol to facilitate transfection with 20 pmol/μl AKAPAkap13 siRNA (*sense strand* 5′-GGC CUG UUC CUC AUC AGU ATT-3′; *antisense strand* 5′UAC UGA UGA GGA ACA GGC CTT-3′) or 20 pmol/μl All Stars Negative (ASN) control (Qiagen, Hilden, Germany).

Human COV434 Granulosa Cells: Cells were cultured and seeded at the densities described above. When the cells were approximately 30–50% confluent, the medium was changed to a fresh complete medium. Xtreme gene (Roche, Cat# 04476093001) was then applied to the cells according to the manufacturer's protocol to facilitate transfection. SiRNA and control sequences were as used for primary murine GC transfection. After siRNA transfection, FSH treatment was performed as described below.

Plasmids—A cDNA encoding the N-terminal coding sequences of *AKAP13* and overlapping with the previously published *BRX* cDNA sequence (Genbank entry AF126008) was amplified from a human mammary gland Marathon-Ready™ cDNA library (Clontech) and sub-cloned into an expression construct for Brx [25]. As an empty construct control, the complete cDNA sequence encoding *AKAP13* was subcloned into a pcDNA4/ HisMaxC (InVitrogen) expression vector to generate HMax-AKAP13 and sequenced. The FSH receptor (FSHR) was a wildtype N-terminal 3xHA-tagged human putative purinergic receptor FKSG79 cloned into pcDNA3.1 + (Invitrogen) at EcoRI (5′) and XhoI (3′). The FSHR vector was obtained from the cDNA Resource Center (www.cdna.org, GenBank accession number AY429104). COV434 cells express FSHR endogenously but since it is uncoupled from downstream signaling, it was transfected into the cells. Exoenzyme Clostridium botulinum (C3) transferase is an ADP ribosyl transferase protein

that specifically inhibits RhoA through ribosylation at asparagine residue 41 thus preventing activation of RhoA by RhoGEF and was obtained commercially (Cytoskeleton, Inc. #CT03-A). The CRE-luciferase reporter, pGL4.29(*luc2P*/CRE/Hygro), was obtained from Promega (Promega Corporation, Madison, WI). To construct the CYP19A1-PII (aromatase) reporter, we amplified the I.3-PII region from human chromosomal DNA, sequenced it, digested it with KpnI and HindIII, and sub-cloned it into the commercially available luciferase expression vector pGL4.25[luc2/minP] (Promega Corporation, Madison, WI). Recombinant clones were isolated, sequenced, and activity was assessed by transient transfection into the DC3 rat GC line.

Transfection, Cell Lysis, and Luciferase Assay—Cells were cultured and seeded at a density of 2.0 to 2.5 × 10^5 cells/well as described above. After reaching 50% confluency, cells were transfected with expression constructs using FuGENE-6™ (Roche Molecular Biochemicals), as described by the manufacturer, and serum-starved overnight. Four to 28 h after transfection, FSH, FSK, or H89 treatment was performed as described below. In experiments using A13 or A02, these treatments were added immediately after transfection. Cells were then harvested, cell lysates prepared, and luciferase activity was assessed using Firefly Luciferase kit (Promega, USA) per manufacturer recommendations. CRE and CYP19A1-PII luciferase (CRE-luc and CYP19A1-luc, respectively) activity was measured in relative light units (RLU) by a CLARIOstar Microplate Reader (BMG Labtech, USA) and normalized using MTS Solution (Promega, USA) or protein concentrations with Precision Red Advanced Protein assay (Cytoskeleton, Inc.) per manufacturer's instruction.

A13, A02, FSH, Forskolin, and H89 Treatment—The small molecules A13 and A02 were identified by virtual screening and are known to alter the Rho-GEF activity of AKAP13 [39]. A13 (ZINC09659342, ChemBridge, USA, catalog #7390017) is a small protein–protein interaction inhibitor of AKAP13, and A02 (ZINC08595092, Ambinter, France, Cat # Amb20267665) is a small protein–protein interaction activator of AKAP13. Briefly, both interact with the DH domain in the GEF region of AKAP13. A13 blocks Rho activation by AKAP13. In contrast, A02 binds to the GEF region of AKAP13 and increases Rho activity. COV434 cells were seeded as above for 1 day, and the media was changed to serum-free media on the second day. On the third day, cells were transfected with CYP19A1-PII-luc reporter construct and treated with 10 μM A13, 10 μM of A02, or DMSO vehicle control. Four hours later, 0.9% NaCl or 1 IU/μl FSH (Gonal F, Merck Serono), was added as a treatment. After 24 h, cells were lysed, assayed for luciferase activity, and normalized with an MTS assay.

For experiments analyzing the effect of treatment with FSH (i.e., siRNA knockdown, western blot, and luciferase assays), COV434 cells were grown to 40–50% confluency and maintained in serum complete media for 48 h. On the third day, the media was changed to serum-free culture media and immediately afterward cells were transfected with either CRE-luc or CYP19A1-PII-luc reporter constructs. Twenty-four hours later, cells were treated with 1 IU/μl FSH, 10 μM Forskolin (FSK) (Sigma, F6886), or 10 μM H89 (Cayman, 10,010,556). Control cells were either treated with fresh serum-free media lacking FSH or with 10 μM of DMSO when compared to FSK or H89 treatment. For luciferase assays, cells were treated

for 24 h prior to harvesting. In western blot experiments, cells were treated with 1 IU/μl FSH for 10 to 60 min prior to harvesting.

RNA Isolation, cDNA Synthesis, and RT-qPCR—Total RNA was isolated from the whole mouse ovary stored in RNALater (Ambion Cat. #AM7021) at − 20 °C and from GCs using the RNeasy Mini Kit (Qiagen, Cat # 74034) according to the manufacturer's protocol. Subsequently, complementary DNA (cDNA) was derived using Biorad iScript cDNA Synthesis Kit (Bio-Rad, Cat. #170-8891) according to the manufacturer's instructions for RNA from whole murine ovaries and from COV434 GCs. Superscript III (Invitrogen, Cat # 18080-051) was used to synthesize cDNA from RNA isolated from primary murine GC cultures, also according to the manufacturer's protocol.

Quantitative real-time PCR (RT-qPCR) reactions were performed using SYBR Green PCR Master Mix (Applied Biosystems) in a Bio-Rad CFX96 Touch™ real-time PCR detection system (Bio-Rad, Hercules, CA) and LightCycler96 (Roche) with a total volume of 20 μl per reaction mixture prepared in 96-well optical reaction plates (BioRad). The primer sequences used for mouse were *akap13* mRNA [*forward*: CGGAAGA AG CTGG TG CGC GA; *reverse*: CTG CTT GAA CCT CTT TCA GCC], aromatase mRNA [*forward* 5′-CCA TCA TGG TCC CGG AAA C-3′; *reverse* 5′-GGC CCAT GATCAG CA GAAG T-3 ′], and *LHR* mRNA [*forward* 5′-CCT TGT GGG TGT CAG CAG TTAC-3′; *reverse* 5′-TTG TGA CAG AGT GGA TTC CACAT-3′]. Aromatase and *LHR* primer sequences were as previously described [23]. Primers used for human (i.e., mRNA derived from COV434 cells) were *AKAP13* mRNA [*forward*: 5′–AGA AGG AGT CTC TGG TGG AT-3′; *reverse* 5′-ACA GAC TGG TTA TGT TGC CCA CAA-3′] and *LHR* mRNA [*forward*: 5′–GCC ATCA AGAGAA AC ATTT GT CAA - 3′; *reverse* 5′-TTTCTA AAA GCA CAG CAG TGGCT-3′]. Aromatase primers were identical for the mouse and human.

A standard reaction mixture contained SsoAdvanced SYBR Green Supermix (Cat. #172-5260) 10 μl of SsoAdvanced SYBR Green Supermix, 1 μl of each primer, 2 μl of cDNA template (10–20 ng as optimized), and 6 μl of RNase/DNase-free water. Common thermal cycling parameters (2 min at 50 °C, 15 min at 95 °C, 40 cycles of 15 s at 94 °C, 35 s at 60 °C, and 35 s at 72 °C) were used to amplify each transcript. Melting-curve analyses were performed to verify product identity. Samples were run in duplicate for primary murine cultures and in triplicate for COV434 and were expressed relative to 18S and GAPDH to normalize for cDNA variability between samples. Relative fold change in target mRNAs was quantified using the Delta-Delta C_T method.

Western Blot and Co-Immunoprecipitation

Antibodies and Antisera—A peptide corresponding to the AKAP13 protein (CREKEK-DKIKEKEKDS KEKEKDKKTLNGHTF) was used to generate polyclonal antiserum 6969 using standard techniques, and binding to AKAP13 was confirmed using an enzyme-linked immunosorbent assay (Covance Laboratories, Sterling, VA) [40]. CREB, phospho-CREB (Ser133), and SMAD2 (SMAD family member 2) antibodies were obtained from Cell Signaling Technology (9197, 91,978, and 3122, respectively).

SDS PAGE Gel Electrophoresis and Transfer—Cells were cultured and seeded as above. In experiments where AKAP13 was overexpressed, at 50% confluency, cells were transfected AKAP13 expression construct or HMax empty control construct as above and harvested in a buffer containing 20 mM Tris (pH 7.4), 150 mM NaCl, 5 mM EDTA, Complete™ protease inhibitors (Roche Molecular Biochemicals), 1% Triton X-100, and 0.5% sodium deoxycholate and lysed by sonication. Protein concentrations in lysates were determined with a BCA protein assay kit (Pierce), as described by the manufacturer. Equal amounts of protein were resolved by electrophoresis on SDS–polyacrylamide gels. Proteins were transferred to nitrocellulose by semi-dry electroblotting. Membranes were blocked in Tris-buffered saline (pH 7.4) containing 0.05% Tween-20 and 5–10% nonfat dry milk for 30 min and then incubated with primary antibodies against CREB proteins, phospho-CREB (Ser 133) phosphor-specific antibody (1:1000), and total CREB antibody (1:1000) overnight in 4 °C. The next day, detection of HRP activity by enhanced chemiluminescence was performed with SuperSignal™ West Pico PLUS Chemiluminescent Substrate (Thermo Fisher Scientific, USA) in an Azure Imager c300 system (Azure Biosystems, USA). The band intensity was quantified using ImageJ software (version 1.52a).

Co-Immunoprecipitation—COV434 cells were harvested in IP Lysis Buffer (Pierce, Thermo Scientific, 87787) with protease and phosphatase inhibitors (Cell Signaling Technology, 5872) and lysates formed. Protein concentration was determined as above. An affinity-purified polyclonal antiserum against AKAP13 (6969) was bound to magnetic Dynabeads protein A (Invitrogen). Lysates were incubated with the anti-sera bound Dynabeads for 1 h at 4 °C, and the target antigen was eluted and processed per the manufacturer's recommendation for SDS PAGE electrophoresis and western blotting against CREB1 antibody. SMAD2 antibody served as an isotype negative control.

Statistical Analysis

Statistical analyses were performed using Prism 5 software (GraphPad Software, Inc, La Jolla, CA). Results of assays and sample values are reported as mean ± standard error of the mean (SEM). Student's *t*-tests were used to determine statistically significant differences as appropriate. A *p*-value less than 0.05 ($p < 0.05$) was considered statistically significant.

Results

Overexpression of AKAP13 Increased Activity of Aromatase Reporter

To test the hypothesis that AKAP13 facilitates the FSH-dependent gene activation in GCs, we performed a series of experiments in an in vitro model of gonadotropin signaling using COV434 GCs. GCs were treated with FSH, and CYP19A1-PII-luc reporter activity was compared in GCs transfected with AKAP13 expression construct versus a control. We found a significantly increased activation of 1.75-fold in aromatase reporter activity in GCs transfected with AKAP13 and treated with 1 IU of FSH, compared to FSH-treated control ($p < 0.001$). We observed that GCs not treated with FSH but transfected with AKAP13 also showed activation of aromatase reporter activity ($p < 0.001$) (Fig. 1a).

Next, we evaluated aromatase reporter activity in the presence of FSK, a molecule known to produce non-specific activation of PKA signaling pathways including those induced by LH and FSH [1]. Transfection of an AKAP13 expression construct into COV434 GCs resulted in a 2.7-fold increase in aromatase reporter activity in untreated cells compared to empty construct control ($p < 0.001$). In FSK-treated GCs, we also observed a significant 2.5-fold increase in aromatase reporter activity in cells transfected with AKAP13 compared to untreated control construct cells ($p < 0.001$) (Fig. 1b). Next, we repeated this experiment with a PKA inhibitor, H89. Treatment with H89 resulted in a significant two-fold reduction in CYP19A1-PII luciferase activity in AKAP13 transfected ($p = 0.0067$) (Fig. 1c). The significant increase in aromatase activity by AKAP13 suggested that AKAP13 might augment CREB1 activity by some mechanism.

AKAP13 Interacts with CREB1 and Was Required for Optimal CREB1 Phosphorylation

To test for a potential interaction between CREB1 and AKAP13, we performed co-immunoprecipitation of AKAP13 and CREB1. The results of these experiments were consistent with the conclusion that AKAP13 binds directly to CREB1 (Fig. 2a) (additional data is given in Online Resource 1). This suggests that AKAP13 may act as a scaffold to bring together PKA and its substrate CREB. It was therefore of interest to examine whether the expression of AKAP13 affects the induction of phospho-CREB1 in response to FSH. Using western blot for CREB phosphorylated at Ser-133, we observed a significant increase in phospho-CREB within 10 min of FSH treatment ($p = 0.03$) in COV434 cells, indicating that CREB1 activation increased with FSH treatment in a time-specific manner (Fig. 2b). We also observed that transfection of AKAP13 expression construct into COV434 cells further increased phosphorylation of CREB (1.25-fold increase) as compared with control construct (1.0-fold increase) (Fig. 2c). We next used AKAP13-targeted siRNA to evaluate the role of *AKAP13* knockdown on FSH induction of phospho-CREB. In the COV434 cell model, siRNA directed against *AKAP13* resulted in a 50–85% knockdown of *AKAP13*, as measured with RT-qPCR ($p = 0.05$) (Fig. 2d). Next, we measured the amount of activated phospho-CREB produced in COV434 cells after exposure to tittered doses of FSH, both with and without *AKAP13*-targeted siRNA present. Relative CREB1 phosphorylation increased nearly two-fold with FSH treatment in cells transfected with control siRNA, while relative CREB1 phosphorylation levels in cells transfected with *AKAP13*-directed siRNA were reduced, and the effect was not reversed with FSH treatment ($p = 0.05$). The observed decrease was also time-specific, reaching the highest significance after 60–120 min of FSH treatment (Fig. 2e). As a control, we used a CRE-luc reporter assay to assess CREB1 phosphorylation. Consistent with a role of AKAP13 in CREB phosphorylation (Fig. 2f), overexpression of AKAP13 significantly augmented FSH-dependent CRE-luc activity, from 6.9-fold with the control construct, to 18.5-fold with AKAP13 ($p < 0.001$) (Fig. 2f). Taken together, these findings suggest that AKAP13 increases phosphorylation of CREB, and the effect requires AKAP13.

A13 and C3 Treatments Reduced AKAP13-Dependent CYP19A1 and CRE Reporter Activity

To determine which regions of AKAP13 were required for FSH signaling, we measured AKAP13-dependent CYP19A1-PII-luc activity after treatment with AKAP13 inhibitors that targeted different regions in the protein. We found that treatment with the AKAP13 RhoGEF

inhibitor A13 in COV434 cells resulted in a 92% decrease in aromatase reporter activity compared to vehicle (DMSO) treated controls ($p < 0.001$). This effect was not reversed with FSH treatment and aromatase reporter activity remained significantly reduced ($p < 0.001$) (Fig. 3a). Interestingly, treatment with AKAP13 RhoGEF activator A02, greatly augmented FSH-dependent aromatase reporter activity by 121% compared to DMSO treated controls ($p < 0.001$) (Fig. 3a). In support of a requirement for GEF activity in the increased response, the RhoA inhibitor C3 exoenzyme transferase also reduced AKAP13-dependent CRE-luciferase activity by 44% compared to empty construct controls ($p = 0.0037$) and by 63% ($p < 0.001$) compared to vehicle-treated cells over-expressing AKAP13 (Fig. 3b).

AKAP13 Was Required for Optimal Aromatase and LHR Transcripts in Response to FSH

To test the hypothesis that AKAP13 facilitates the production of aromatase and LHR in GCs, we performed a series of knockdown experiments using primary murine GCs as well as COV434 cells. In FSH-treated COV434 cells, a significant induction (~ eightfold) of aromatase mRNA was observed in control cells (Fig. 4a). In contrast, siRNA directed against *AKAP13* resulted in a significant knockdown of aromatase induction by FSH ($p < 0.001$) (Fig. 4a). In similar experiments, FSH-induced *LHR* expression was significantly impaired by 50% in COV434 cells treated with siRNA against *AKAP13* compared to control siRNA ($p < 0.001$) (Fig. 4b). These findings were confirmed in primary murine GCs. As in COV434 cell experiments, we used siRNA knockdown of *Akap13* to assess the function of AKAP13 in primary murine GCs. In primary murine cultures, we observed a > 80% knockdown of *Akap13* ($p < 0.001$) (Fig. 4c), a 46% decrease in basal aromatase mRNA expression ($p = 0.03$) (Fig. 4d), and a 32% reduction in FSH-induced *LHR* expression ($p = 0.02$) with siRNA directed against *Akap13* as compared with control siRNA (Fig. 4e) (additional data is given in Online Resource 1).

Discussion

These findings suggest that AKAP13 affects FSH-dependent activation of the PKA pathway through a physical interaction with CREB, resulting in increased CREB1 phosphorylation in a time-dependent manner. Furthermore, augmented activation of CREB1 required the RhoGEF region of AKAP13, revealing additional insight into the mechanisms involved. These data suggest, for the first time, a direct link between AKAP13 and CREB1 activation as a mechanism for the augmentation of FSH-mediated GC signaling pathways.

Gametogenesis in the human female involves a complex series of events culminating in follicular development and ovulation, driven primarily by the ability of the GC to respond to FSH. Our previous studies of AKAP13 protein expression in the human ovary showed AKAP13 expression in thecal cells and the induction of expression in GCs of preovulatory follicles and corpus lutein [20, 25, 32, 41] leading us to postulate that AKAP13 could be involved in FSH-dependent signaling and the production of downstream targets genes, such as *CYP19A1* and *LHR*. Recently, Zhang et al. [42] reported that a 16-bp indel locus on *AKAP13* was associated with litter size in goats and a marker for fertility, which aligns with our results on the involvement of AKAP13 in GC function and ovulation. Our hypothesis that AKAP13 interacts with PKA to activate CREB1 as a mechanism for

inducing aromatase and *LHR* expression in response to FSH is supported by the fact that the aromatase promoter contains several CRE-like CREB binding domains involved in gene transcription. Additionally, CREB1 has been previously implicated in follicular growth and ovulation [43]. Evidence supports this interaction, because FSH is known to regulate the expression of the RII subunits of PKA in the ovary [11–13], and RII isoform-specific AKAPs have been previously demonstrated to regulate the subcellular distribution of type II PKA in response to FSH [35, 44]. Gu et al. previously reported that AKAP95 is involved in CREB phosphorylation and expression of aromatase in GCs [45], which renders the FSH-AKAP13-PKA-CREB-aromatase pathway biologically plausible and akin to the role reported for AKAP95 previously.

In addition to its PKA RII binding domain, AKAP13 has a GEF domain that confers selective RhoGEF activity to the anchoring protein and mediates its activation [44]. It has been established that PKA can directly inhibit RhoA through phosphorylation of serine residue 188 in its C-terminal region [46, 47]. PKA has also been shown to directly deactivate the function of AKAP13's RhoGEF domain through the recruitment of the protein 14-3-3, suggesting that AKAP13 serves as an anchor between the PKA and RhoA signaling pathways [48]. We report, for the first time, that inhibition of AKAP13's RhoGEF functionality by C3 transferase and A13 can reduce PKA activation of CREB1 (Fig. 3b). The RhoA signaling pathway is important in cell cycle progression, actin polymerization, cytoskeleton remodeling, cell proliferation, and migration. A majority of RhoA is sequestered in the cytoplasm (> 95%) where it remains in a mostly inactive state coupled with Rho-guanine dissociation inhibitors (RhoGDIs) [49]. As AKAP13 is predominantly within the cytoplasm, it could function as an additional anchor of RhoA to serve as a substrate target for PKA thus regulating downstream signaling of FSH.

Moreover, our finding that AKAP13 augments FSH-induced production of key protein products necessary for follicular development is substantiated by previous studies of AKAP proteins. Specifically, Carr et al. [44] previously suggested that the AKAP family of proteins is involved in regulating the transition from preantral to preovulatory follicles, based upon observations that certain AKAP proteins and PKA have different expression patterns in preantral follicles as compared with preovulatory follicles. Since then, AKAP MAP2D was found to be specifically involved in GC function in preovulatory follicles [50]. Future studies may probe how PKA RII and RhoGEF domains may coordinate FSH-mediated CREB activation in GCs. The involvement of RhoA is interesting given the roles of Hippo and mechanical signaling in the ovary. Actin regulation via Rho GTPase activity has been shown to activate Hippo signaling inhibition via yes-associated protein (YAP)/transcription coactivator with PDZ-binding motif activity and affect primordial follicle activation leading to follicular growth and human embryonic stem cell survival [30, 51]. *YAP1* has also been implemented in susceptibility to PCOS where ovarian enlargement is a common finding [52]. AKAP13's activation of Rho can lead to stimulation of YAP and growth factors important for follicular growth in GCs. Maher et al. found that treatment of COV434 GCs with A13 and A02 led to a downregulation and upregulation, respectively, in YAP-responsive gene expression suggesting a role for AKAP13-dependent Rho activation in the Hippo signaling pathway [41].

A proposed model based upon these data is that during follicular development, FSH binding to the FSHR on GCs, results in the activation of PKA, and that a direct physical interaction between PKA and AKAP13 (via its RII regulatory subunit binding domain) serves as a mechanism for phosphorylation of CREB1 (Fig. 5a). CREB1 activation, in turn, activates aromatase and LHR production in growing follicles. This mechanism suggests that AKAP13 serves as a mediator in FSH-induced expression of aromatase and *LHR* via the PKA-CREB pathway (Fig. 5a). Interestingly, the unique RhoGEF domain of AKAP13 was also required for optimal phosphorylation of CREB1 highlighting the complexity of downstream FSH signaling in GCs (Fig. 5b).

In conclusion, we found that FSH-mediated CREB1 activation in GCs was augmented by AKAP13 and the formation of a signaling module involving both the PKA and RhoA pathways. These findings provide insight into the intermediary steps in the FSH-dependent signaling pathways critical to follicular development. This knowledge could inform future studies designed to target the interaction between AKAP13 and CREB1 in the ovary.

Supplementary Material

Refer to Web version on PubMed Central for supplementary material.

Acknowledgements

The authors thank Joshua T. Brennan, M.S., MPH and Md Soriful Islam, Ph.D.

Funding

Research reported in this publication was supported in part by the Howard and Georgeanna Jones Endowment; National Institutes of Health Grant ZIA-HD-008737-11 (to J.H.S.); the Eunice Kennedy Shriver National Institute of Child Health & Human Development of the National Institutes of Health under Award Number K12-HD-103036 (to K.C.V); the Society for Reproductive Investigation and Bayer Discovery Innovation Grant (to K.C.V); the Clinical Research Training Program, a public–private partnership supported jointly by the National Institutes of Health (to K.D. and M.M.); the Johns Hopkins University School of Medicine Predoctoral Research Program for Medical Students (Dean's Year of Research) (to A.S.C.); NIH ZIA-HD-008985 (to J.Y.M.); and the Edward E. Wallach Research Award (to J.Y.M.).

References

1. Hunzicker-Dunn M, Maizels ET. FSH signaling pathways in immature granulosa cells that regulate target gene expression: Branching out from protein kinase A. Cell Signal. 2006;18(9):1351–9. 10.1016/j.cellsig.2006.02.011. [PubMed: 16616457]
2. Law NC, Weck J, Kyriss B, Nilson JH, Hunzicker-Dunn M. Lhcgr Expression in granulosa cells: roles for PKA-phosphorylated β-catenin, TCF3, and FOXO1. Mol Endocrinol. 2013;27(8):1295–310. 10.1210/me.2013-1025. [PubMed: 23754802]
3. Escamilla-Hernandez R, Little-Ihrig L, Orwig KE, Yue J, Chandran U, Zeleznik AJ. Constitutively active protein kinase A qualitatively mimics the effects of follicle-stimulating hormone on granulosa cell differentiation. Mol Endocrinol. 2008;22(8):1842–52.10.1210/me.2008-0103. [PubMed: 18535249]
4. Puri P, Little-Ihrig L, Chandran U, Law NC, Hunzicker-Dunn M, Zeleznik AJ. Protein kinase A a master kinase of granulosa cell differentiation. Sci Rep. 2016;6(1):28132. 10.1038/srep28132. [PubMed: 27324437]
5. Vassart G, Smits G, Campillo M, et al. Glycoprotein hormone receptors: determinants in leucine-rich repeats responsible for ligand specificity. EMBO J. 2003;22(11):2692–703. 10.1093/emboj/cdg260. [PubMed: 12773385]

6. Beebe SJ, Segaloff DL, Burks D, Beasley-Leach A, Limbird LE, Corbin JD. Evidence that cyclic adenosine 3',5'-monophosphate-dependent protein kinase activation causes pig ovarian granulosa cell differentiation, including increases in two type II subclasses of this kinase. Biol Reprod. 1989;41(2):295–307. 10.1095/biolreprod41.2.295. [PubMed: 2553142]
7. DeManno DA, Cottom JE, Kline MP, Peters CA, Maizels ET, Hunzicker-Dunn M. Follicle-stimulating hormone promotes histone H3 phosphorylation on serine-10. Mol Endocrinol. 1999;13(1):91–105. 10.1210/mend.13.1.0222. [PubMed: 9892015]
8. Hillier SG, Zeleznik AJ, Ross GT. Independence of steroidogenic capacity and luteinizing hormone receptor induction in developing granulosa cells. Endocrinology. 1978;102(3):937–46. 10.1210/endo-102-3-937. [PubMed: 217610]
9. Welch EJ, Jones BW, Scott JD. Networking with AKAPs: context-dependent regulation of anchored enzymes. Mol Interv. 2010;10(2):86–97. 10.1124/mi.10.2.6. [PubMed: 20368369]
10. Skalhegg BS, Tasken K. Specificity in the cAMP PKA signaling pathway differential expression regulation and subcellular localization of subunits of PKA. Front Biosci. 2000;5(3):678. 10.2741/A543.
11. Oyên O, Myklebust F, Scott JD, et al. Subunits of cyclic adenosine 3',5'-monophosphate-dependent protein kinase show differential and distinct expression patterns during germ cell differentiation: alternative polyadenylation in germ cells gives rise to unique smaller-sized mRNA species. Biol Reprod. 1990;43(1):46–54. 10.1095/biolreprod43.1.46. [PubMed: 2393692]
12. Richards JS, Haddox M, Tash JS, Walter U, Lohmann S. Adenosine 3′,5′-monophosphate-dependent protein kinase and granulosa cell responsiveness to gonadotropins. Endocrinology. 1984;114(6):2190–8. 10.1210/endo-114-6-2190. [PubMed: 6327238]
13. Ratoosh SL, Richards JS. Regulation of the content and phosphorylation of RII by adenosine 3',5'-monophosphate, follicle-stimulating hormone, and estradiol in cultured granulosa cells. Endocrinology. 1985;117(3):917–27. 10.1210/endo-117-3-917. [PubMed: 2990878]
14. Newhall KJ, Criniti AR, Cheah CS, et al. Dynamic anchoring of PKA is essential during oocyte maturation. Curr Biol. 2006;16(3):321–7. 10.1016/j.cub.2005.12.031. [PubMed: 16461287]
15. Carlone DL, Richards JS. Evidence that functional interactions of CREB and SF-1 mediate hormone regulated expression of the aromatase gene in granulosa cells and constitutive expression in R2C cells. J Steroid Biochem Mol Biol. 1997;61(3):223–31. 10.1016/S0960-0760(96)00206-3. [PubMed: 9365194]
16. Conti M Specificity of the cyclic adenosine 3′,5′-monophosphate signal in granulosa cell function. Biol Reprod. 2002;67(6):1653–61. 10.1095/biolreprod.102.004952. [PubMed: 12444038]
17. Maizels ET. Follicle Stimulating Hormone (FSH) Activates the p38 mitogen-activated protein kinase pathway, inducing small heat shock protein phosphorylation and cell rounding in immature rat ovarian granulosa cells. Endocrinology. 1998;139(7):3353–6. 10.1210/en.139.7.3353. [PubMed: 9645711]
18. Wayne CM, Fan H, Cheng X, Richards JS. Follicle-stimulating hormone induces multiple signaling cascades: evidence that activation of Rous sarcoma oncogene, RAS, and the epidermal growth factor receptor are critical for granulosa cell differentiation. Mol Endocrinol. 2007;21(8):1940–57. 10.1210/me.2007-0020. [PubMed: 17536007]
19. Cottom J, Salvador LM, Maizels ET, et al. Follicle-stimulating hormone activates extracellular signal-regulated kinase but not extracellular signal-regulated kinase kinase through a 100-kDa Phosphotyrosine Phosphatase. J Biol Chem. 2003;278(9):7167–79. 10.1074/jbc.M203901200. [PubMed: 12493768]
20. Rubino D, Driggers P, Arbit D, et al. Characterization of Brx, a novel Dbl family member that modulates estrogen receptor action. Oncogene. 1998;16(19):2513–26. 10.038/sj.onc.1201783. [PubMed: 9627117]
21. Scott JD, Wong W. AKAP signalling complexes: focal points in space and time. Nat Rev Mol Cell Biol. 2004;5(12):959–70. 10.1038/nrm1527. [PubMed: 15573134]
22. Feliciello A, Gottesman ME, Avvedimento EV. The biological functions of A-kinase anchor proteins. J Mol Biol. 2001;308(2):99–114. 10.1006/jmbi.2001.4585. [PubMed: 11327755]

23. Zheng Y, Olson MF, Hall A, Cerione RA, Toksoz D. Direct involvement of the small GTP-binding protein Rho in lbc oncogene function. J Biol Chem. 1995;270(16):9031–4. 10.1074/jbc.270.16.9031. [PubMed: 7721814]
24. Diviani D, Soderling J, Scott JD. AKAP-Lbc anchors protein kinase A and nucleates Galpha 12-selective Rho-mediated stress fiber formation. J Biol Chem. 2001;276(47):44247–57. 10.1074/jbc.M106629200. [PubMed: 11546812]
25. Driggers PH, Segars JH, Rubino DM. The proto-oncoprotein Brx activates estrogen receptor β by a p38 mitogen-activated protein kinase pathway. J Biol Chem. 2001;276(50):46792–7. 10.1074/jbc.M106927200. [PubMed: 11579095]
26. Kino T, Souvatzoglou E, Charmandari E, et al. Rho family guanine nucleotide exchange factor Brx couples extracellular signals to the glucocorticoid signaling system. J Biol Chem. 2006;281(14):9118–26. 10.1074/jbc.M509339200. [PubMed: 16469733]
27. Ng SS, Jorge S, Malik M, et al. A-Kinase Anchoring Protein 13 (AKAP13) Augments progesterone signaling in uterine fibroid cells. J Clin Endocrinol Metab. 2019;104(3):970–80. 10.1210/jc.2018-01216. [PubMed: 30239831]
28. Maravet Baig K, Su S, Mumford SL, et al. Mice deficient in AKAP13 (BRX) develop compulsive-like behavior and increased body weight. Brain Res Bull. 2018;140:72–9. 10.1016/j.brainresbull.2018.04.005. [PubMed: 29653158]
29. Koide H, Holmbeck K, Lui JC, et al. Mice deficient in AKAP13 (BRX) are osteoporotic and have impaired osteogenesis. J Bone Miner Res. 2015;30(10):1887–95. 10.1002/jbmr.2534. [PubMed: 25892096]
30. Ohgushi M, Minaguchi M, Sasai Y. Rho-signaling-directed YAP/TAZ activity underlies the long-term survival and expansion of human embryonic stem cells. Cell Stem Cell. 2015;17(4):448–61. 10.1016/j.stem.2015.07.009. [PubMed: 26321201]
31. Qiao Z, Jiang Y, Wang L, Wang L, Jiang J, Zhang J. Mutations in KIAA1109, CACNA1C, BSN, AKAP13, CELSR2, and HELZ2 are associated with the prognosis in endometrial cancer. Front Genet. 2019;10:909. 10.3389/fgene.2019.00909. [PubMed: 31787999]
32. Miller BT, Rubino DM, Driggers PH, et al. Expression of brx proto-oncogene in normal ovary and in epithelial ovarian neoplasms. Am J Obstet Gynecol. 2000;182(2):286–95. 10.1016/S0002-9378(00)70213-4. [PubMed: 10694326]
33. Hearns-Stokes R, Mayers C, Zahn C, et al. Expression of the proto-oncoprotein breast cancer nuclear receptor auxiliary factor (Brx) is altered in eutopic endometrium of women with endometriosis. Fertil Steril. 2006;85(1):63–70. 10.1016/j.fertnstert.2005.06.053. [PubMed: 16412732]
34. Alam H, Maizels ET, Park Y, et al. Follicle-stimulating hormone activation of hypoxia-inducible factor-1 by the phosphatidylinositol 3-kinase/AKT/Ras homolog enriched in brain (Rheb)/mammalian target of rapamycin (mTOR) pathway is necessary for induction of select protein markers of follicular differentiation. J Biol Chem. 2004;279(19):19431–40. 10.1074/jbc.M401235200. [PubMed: 14982927]
35. Carr DW, DeManno DA, Atwood A, Hunzicker-Dunn M, Scott JD. Follicle-stimulating hormone regulation of A-kinase anchoring proteins in granulosa cells. J Biol Chem. 1993;268(28):20729–32. 10.1016/S0021-9258(19)36841-3. [PubMed: 8407895]
36. Gong X, McGee EA. Smad3 is required for normal follicular follicle-stimulating hormone responsiveness in the mouse. Biol Reprod. 2009;81(4):730–8. 10.1095/biolreprod.108.070086. [PubMed: 19535790]
37. van den Berg-Bakker Cornelia AM, Hagemeijer A, FrankenPostma EM, et al. Establishment and characterization of 7 ovarian carcinoma cell lines and one granulosa tumor cell line: Growth features and cytogenetics. Int J Cancer. 1993;53(4):613–20. 10.1002/ijc.2910530415. [PubMed: 8436435]
38. Zhang H, Vollmer M, De Geyter M, et al. Characterization of an immortalized human granulosa cell line (COV434). Mol Hum Reprod. 2000;6(2):146–53. 10.1093/molehr/6.2.146. [PubMed: 10655456]

39. Diviani D, Raimondi F, Del Vescovo C, et al. Small-molecule protein-protein interaction inhibitor of oncogenic Rho signaling. Cell Chem Biol. 2016;23(9):1135–46. 10.1016/j.chembiol.2016.07.015. [PubMed: 27593112]
40. Mayers CM, Wadell J, McLean K, et al. The Rho guanine nucleotide exchange factor AKAP13 (BRX) is essential for cardiac development in mice. J Biol Chem. 2010;285(16):12344–54. 10.1074/jbc.M110.106856. [PubMed: 20139090]
41. Maher JY, Islam MS, Yin O, et al. The role of Hippo pathway signaling and A-kinase anchoring protein 13 in primordial follicle activation and inhibition. F&S Science. 2022;3(2):118–29. 10.1016/j.xfss.2022.03.002. [PubMed: 35560009]
42. Zhang X, Yuan R, Bai Y, Yang Y, Song X, Lan X, Pan C. A deletion mutation within the goat AKAP13 gene is significantly associated with litter size. Anim Biotechnol. 2021. 10.1080/10495398.2021.1968418.
43. Zhang P, Wang J, Lang H, et al. Knockdown of CREB1 promotes apoptosis and decreases estradiol synthesis in mouse granulosa cells. Biomed Pharmacother. 2018;105:1141–6. 10.1016/j.biopha.2018.06.101. [PubMed: 30021350]
44. Carr DW, Cutler JRE, Cottom JE, et al. Identification of cAMP-dependent protein kinase holoenzymes in preantral- and preovulatory-follicle-enriched ovaries, and their association with A-kinaseanchoring proteins. Biochem J. 1999;344(2):613–23. 10.1042/0264-6021:3440613. [PubMed: 10567247]
45. Gu Y, Xu W, Zhuang B, Fu W. Role of A-kinase anchoring protein 95 in the regulation of cytochrome P450 family 19 subfamily A member 1 (CYP19A1) in human ovarian granulosa cells. Reprod Fertil Dev. 2018;30(8):1128–36. 10.1071/RD17313. [PubMed: 29397057]
46. Lang P, Gesbert F, Delespine-Carmagnat M, Stancou R, Pouchelet M, Bertoglio J. Protein kinase A phosphorylation of RhoA mediates the morphological and functional effects of cyclic AMP in cytotoxic lymphocytes. EMBO J. 1996;15(3):510–9. 10.1002/j.1460-2075.1996.tb00383.x. [PubMed: 8599934]
47. Ellerbroek SM, Wennerberg K, Burridge K. Serine phosphorylation negatively regulates RhoA in vivo. The J Biol Chem. 2003;278(21):19023–31. 10.1074/jbc.M213066200. [PubMed: 12654918]
48. Diviani D, Abuin L, Cotecchia S, Pansier L. Anchoring of both PKA and 14-3-3 inhibits the Rho-GEF activity of the AKAP-Lbc signaling complex. EMBO J. 2004;23(14):2811–20. 10.1038/sj.emboj.7600287. [PubMed: 15229649]
49. Lang P, Gesbert F, Thiberge JM, et al. Characterization of a monoclonal antibody specific for the Ras-related GTP-bBinding protein Rho A. Biochem Biophys Res Commun. 1993;196(3):1522–8. 10.1006/bbrc.1993.2424. [PubMed: 8250908]
50. Salvador LM, Flynn MP, Avila J, et al. Neuronal microtubule-associated protein 2D is a dual A-kinase anchoring protein expressed in rat ovarian granulosa cells. The J Biol Chem. 2004;279(26):27621–32. 10.1074/jbc.M402980200. [PubMed: 15056665]
51. Kawamura K, Cheng Y, Suzuki N, et al. Hippo signaling disruption and Akt stimulation of ovarian follicles for infertility treatment. Proc Natl Acad Sci USA. 2013;110(43):17474–9. 10.1073/pnas.1312830110. [PubMed: 24082083]
52. Li T, Zhao H, Zhao X, et al. Identification of YAP1 as a novel susceptibility gene for polycystic ovary syndrome. J Med Genet. 2012;49(4):254–7. 10.1136/jmedgenet-2011-100727 [PubMed: 22499345]

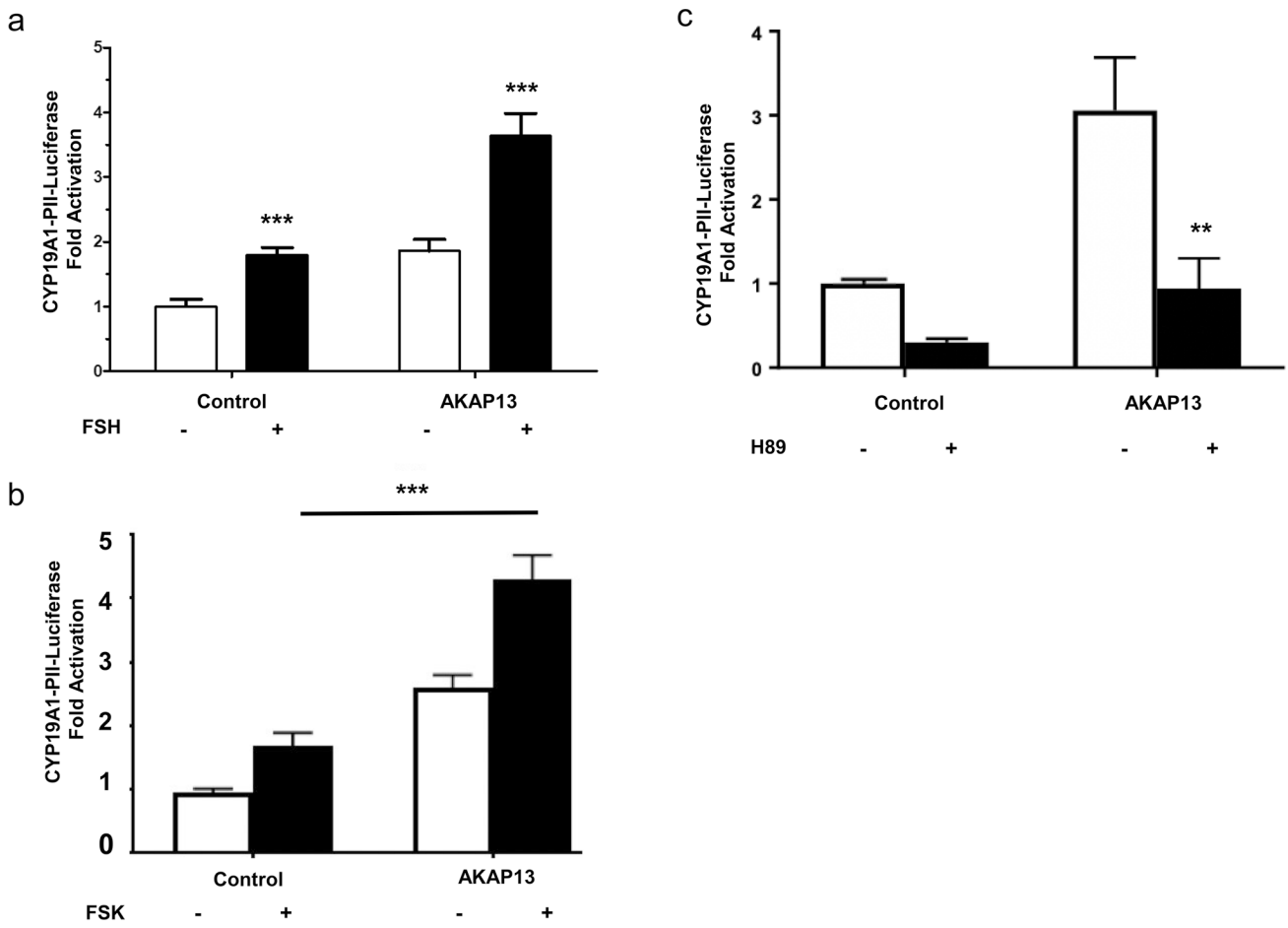

Fig. 1.

Overexpressing AKAP13 increased aromatase reporter activity in granulosa cells. **a** COV434 cells were treated with FSH 1 IU/mL for 24 h, and CYP19A1-PII-luciferase activity was compared between cells transfected with HMax control or AKAP13 expression constructs. FSH treatment increased aromatase promoter activity in cells overexpressing AKAP13 (black bars). The CYP19A1-PII-luciferase activity was significantly increased in untreated cells transfected with AKAP13 as compared with HMax (white bars). **b** Transfection of COV434 cells with AKAP13 expression construct increased aromatase reporter activity by 2.7-fold in untreated cells compared to empty construct control (white bars) and by 2.5-fold in FSK treated cells compared to empty construct control (black bars). **c** Conversely, addition of the PKA inhibitor H89 decreased aromatase reporter activity in AKAP13-transfected COV434 cells by 69% (twofold), returning activation of the aromatase promoter to levels similar to that induced by the empty construct control (***$p < 0.001$, **$p = 0.0067$)

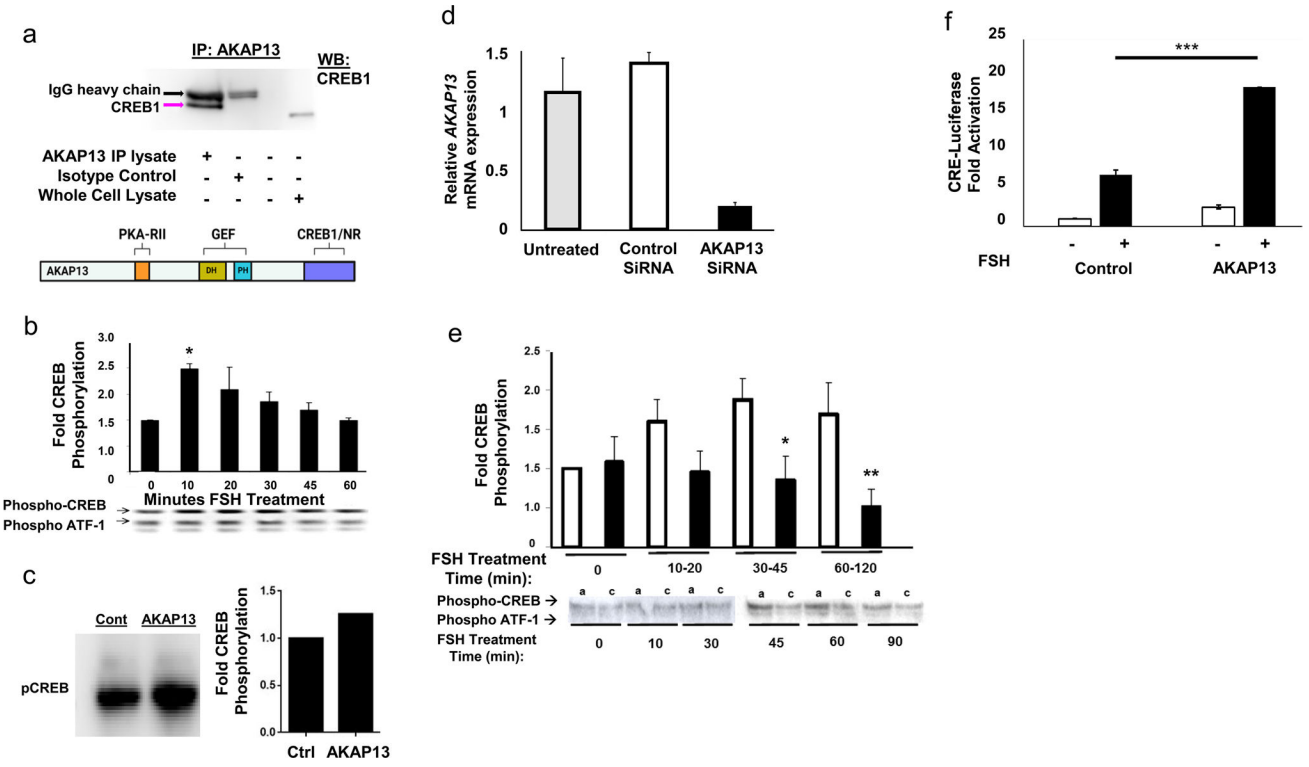

Fig. 2.

AKAP13 interacts with CREB1 and was required for optimal CREB1 phosphorylation. **a** Co-immunoprecipitation of AKAP13 and CREB1. COV434 cell lysates were incubated with Dynabeads™, and AKAP13 immunoprecipitants (IP) were eluted and separated by SDS PAGE electrophoresis followed by western blot (WB) with CREB1 antibody. Co-IP was also performed with an antibody against SMAD2 as a negative isotype control. The pink arrow represents CREB1 at ~ 47 kDa, and the black arrow represents the IgG heavy chain. The schematic of AKAP13 domains was as follows: protein kinase A regulatory unit II (PKA-RII), guanine nucleotide exchange factor (GEF) with DH Dbl-homology and PH Pleckstrin-homology, and nuclear hormone receptor (NR)/CREB1 binding site. **b** Western blot analysis of whole COV434 cell lysates treated with 1 IU/mL FSH for various durations. Band intensity with phospho-CREB antibody (Ser-133) probe (43 kDa) was normalized to band intensity probed with total CREB (43 kDa). Relative CREB phosphorylation peaked by 10 min of FSH treatment ($p = 0.03$ relative to no treatment) and returned to baseline by 45 min of treatment. **c** AKAP13 overexpression increased phosphorylation of CREB by 1.25-fold compared to empty construct (Hmax) control. COV434 cells were transfected with either Hmax (Ctrl) or AKAP13 expression constructs, lysed, and protein lysates electrophoresed by SDS PAGE and western blot for phospho-CREB (pCREB) antibody. **d** Efficient siRNA knockdown of AKAP13 mRNA: analysis of whole cell RNA derived from cultured COV434 cells un-transfected or transfected with AllStars Negative control siRNA or siRNA directed against *AKAP13* demonstrated 50–85% knockdown of *AKAP13* expression, depending on the experiment. **e** Western blot analysis of whole cell lysates of COV434 cells serum starved and transfected with control (AllStars negative, white bars) siRNA or siRNA directed against *AKAP13* (black bars) and treated with 1 IU/mL FSH for durations as shown.

Phospho-CREB band intensity was normalized to that of the total CREB antibody. Relative CREB phosphorylation increased nearly two-fold in cells transfected with control siRNA but did not increase with FSH treatment in cells transfected with *AKAP13* siRNA. Bars represent the mean relative phosphorylation of 3 experiments and error bars = SEM. Data were compared using Student's *t*-test, comparing the same FSH treatment time point in cells transfected with control vs. *AKAP13* siRNA (*$p = 0.05$; **$p = 0.02$). **f** COV434 cells were transfected with either HMAX (control) or AKAP13 expression constructs. Overexpression of AKAP13 significantly augmented FSH-dependent CRE-Luciferase activity, from 6.9-fold with a control to 18.5-fold with an AKAP13 expression construct (***$p < 0.001$)

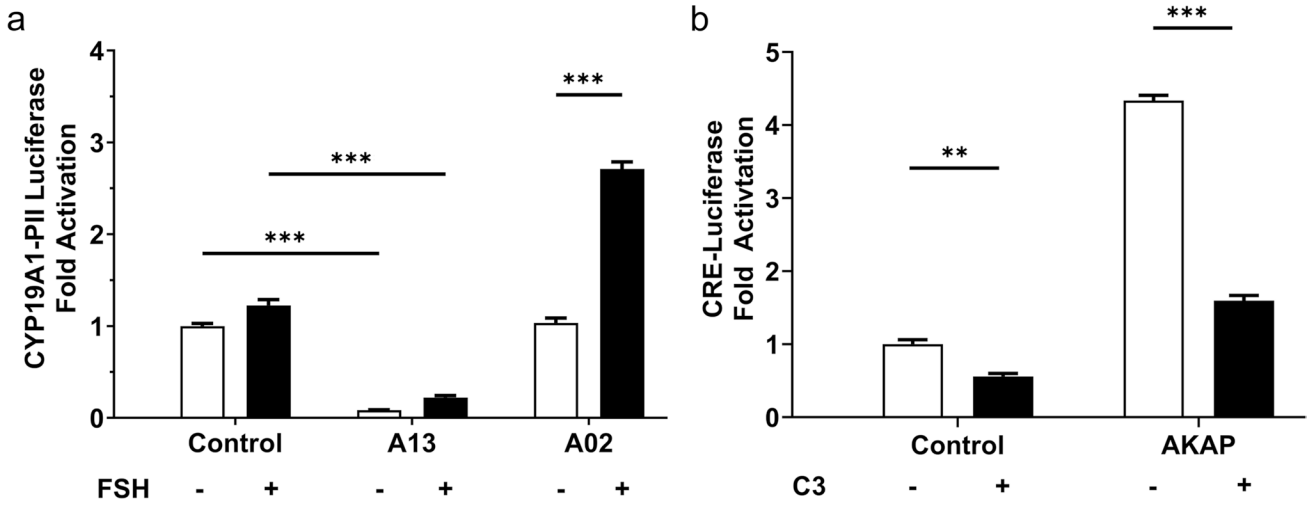

Fig. 3.

A13 and C3 treatments reduced AKAP13-dependent CRE reporter activity while A02 treatment increased CRE reporter activity. **a** COV434 cells transfected with a CYP19A1-PII luciferase reporter construct were treated with DMSO (vehicle control), 10 μM of A13, or 10 μM of A02. Four hours later, 0.9% NaCl (vehicle control) or 1 IU/mL of FSH was added to the media. Cells were harvested 24 h later, and luciferase assays were performed. A13 significantly reduced CYP19A1-PII luc activity by 92% in cells compared to vehicle-treated (DMSO) controls. Addition of FSH did not restore aromatase activity to basal levels with a reduction in aromatase reporter activity by 82% in cells treated with A13. Treatment with the Rho-GEF activator, A02 significantly increased FSH-induced aromatase reporter activity by 121% compared to vehicle control. **b** COV434 cells were transfected with CRE-luc reporter construct, AKAP13 expression construct, HMax empty construct control, C3 transferase, or CEV0 empty construct control. The RhoA inhibitor C3 transferase, significantly reduced CREB reporter activity by 44% compared to empty construct control. C3 transferase also significantly decreased AKAP13-induced CREB activity from 4.3-fold to 1.6-fold, representing a 63% decrease (***$p < 0.001$; **$p = 0.0037$)

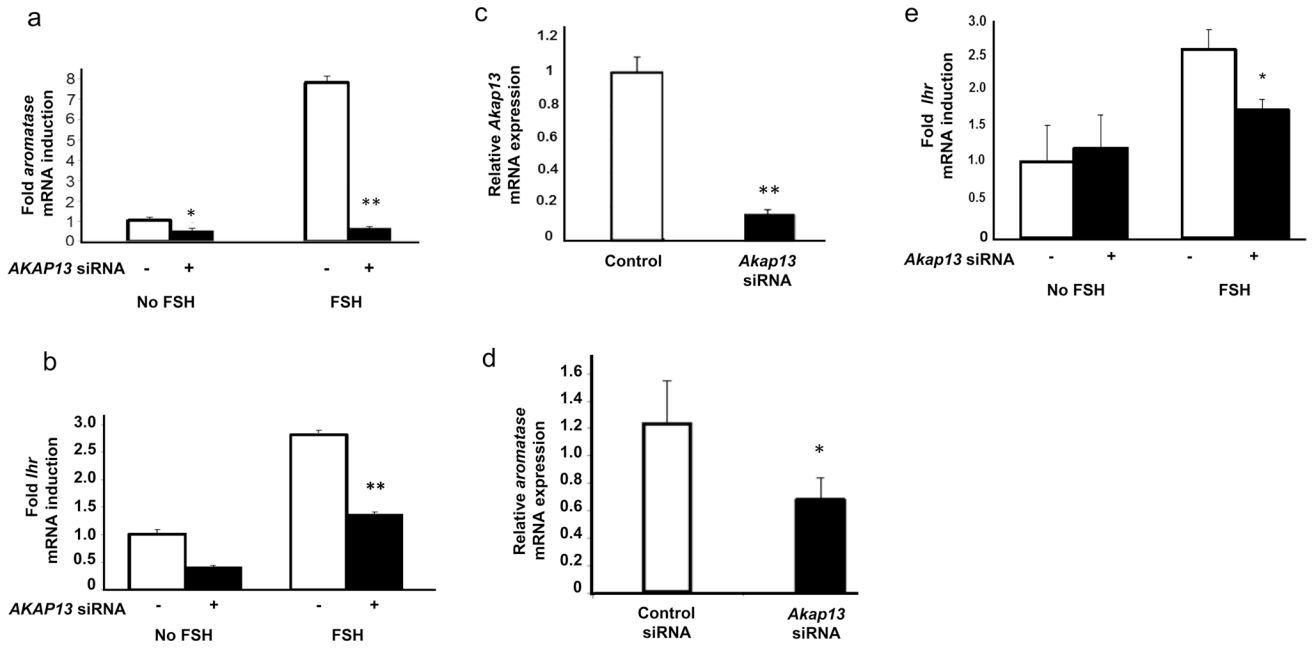

Fig. 4.

AKAP13 was required for optimal aromatase and *LHR* mRNA expression in mammalian granulosa cells. **a** Cultured COV434 cells at 50% confluence were serum starved and transfected with AllStars Negative control siRNA (white bars) or siRNA directed against *AKAP13* (black bars). Cells were treated with serum-free media alone or with 1 IU/mL FSH for ~ 48 h. SiRNA knockdown of *AKAP13* resulted in ~ 50% reduction of basal aromatase message. FSH treatment resulted in nearly eightfold induction of aromatase message in cells treated with control siRNA, and no induction was seen in siRNA-treated cells. **b** qRT-PCR analysis of RNA derived from whole cell extracts transfected with AllStars Negative control siRNA (white bars) or siRNA directed against *AKAP13* (black bars). Following transfection, COV434 Cells were serum starved overnight and either left untreated or treated with 1 IU/mL FSH for ~ 48 h. The induction of luteinizing hormone receptor (*LHR)* with FSH was 2.8-fold. Knockdown of *AKAP13* reduced both basal *LHR* expression and induction of *LHR* message at 48 h treatment by 50%. Primary murine GCs were grown to approximately 50% confluency, serum starved in Opti-MEM for 24 h, then transfected with *Akap13* siRNA (black bar) or AllStars Negative control siRNA (white bar). Twenty-four hours following siRNA treatment, total cellular RNA was extracted, and > 80% decrease in *Akap13* expression was noted. **c** qRT-PCR demonstrated efficient siRNA knockdown of Akap13. **d** Primary murine GCs were serum starved in Opti-MEM at 50% confluence, then transfected with *Akap13* siRNA (black bar) or AllStars Negative control siRNA (white bar) for 24 h. Basal levels of aromatase mRNA were reduced significantly in cells treated with siRNA directed against *Akap13* versus those transfected with control siRNA. **e** qRT-PCR analysis of RNA derived from whole cell extracts transfected with AllStars Negative control siRNA (white bars) or siRNA directed against *Akap13* (black bars). Knockdown of A*kap13* reduced induction of *Lhr* transcripts by 32% at 48-h FSH treatment in primary murine GCs. Error bars = standard error of the mean of triplicate reactions and are representative of data from three experiments (*$p < 0.04$; **$p < 0.001$)

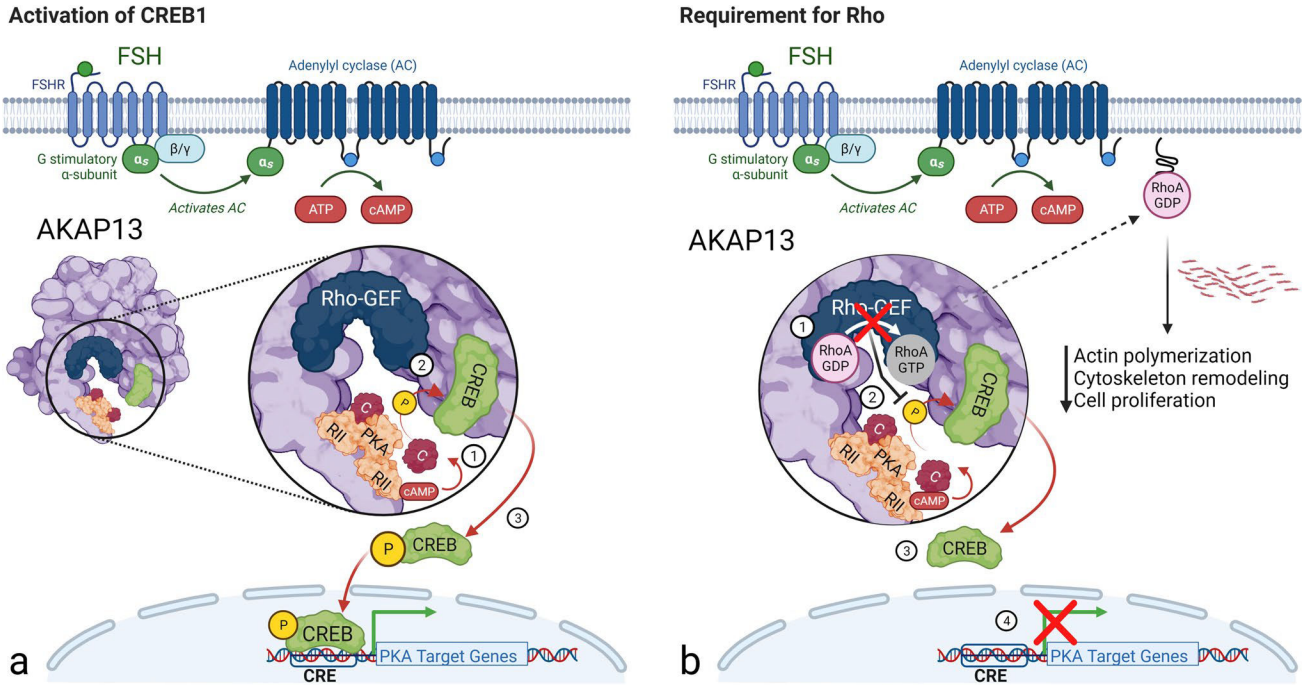

Fig. 5.

Proposed signaling pathway. **a** FSH activates adenylate cyclase (AC) which in turn converts ATP to cAMP (cyclic AMP) (1). cAMP binds to the regulatory subunit II (RII) of PKA releasing the catalytic (C) subunit which promotes phosphorylation (P) of CREB (2). Phosphorylated CREB travels to the nucleus where it binds cAMP response element (CRE)-like sequences in the promoter region of PKA target genes to promote gene activation and transcription (3). **b** The AKAP13 signaling scaffold with the RhoGEF domain activates RhoA to promote actin polymerization, cytoskeleton remodeling, cell proliferation, and migration. Inhibition of the Rho-GEF domain of AKAP13 by A13 (1) inhibits PKA phosphorylation of CREB (2), CREB nuclear transport (3), and subsequent transcription of PKA target genes (4). Created with BioRender.com